Journal of Offshore Structure and Technology
Research paper
Vol 11, issue 1,2024
Receiving date:10-5-2024
Acceptance- 20-05-2024
Publication 21-05-2024

Analysis of new Floating Offshore Wind Turbine under drag force operation

Carlos Armenta Déu [1]; Diego Piqueras Sanz 2*
masterenergyucm@gmail.com,
1Professor, Department of Matter Structure, Thermal Physics and Electronics, Faculty of Physical Sciences, Complutense University of Madrid, 28040 Madrid, Spain

21Professor, Department of Matter Structure, Thermal Physics and Electronics, Faculty of Physical Sciences, Complutense University of Madrid, 28040 Madrid, Spain

Abstract

The goal of this paper is the study and analysis of a new type of floating offshore wind turbine (FOWT), which operates under drag force instead of lifting force as the conventional FOWT. We simulate the wind turbine operation modifying the pitch angle to faithfully reproduce the behavior when submitted to waves' movement. The analysis of the wind turbine performance is developed in a model at laboratory scale to control the power generation under variable operating conditions. Tests run for variable wind speed in the available wind tunnel range, from 0 to 72 km/h. We determine the efficiency of the new wind turbine model determining the output power for setup wind speed, and comparing the results with those obtained from a conventional model, lifting type, of similar characteristics under identical operating conditions. The tests results show that the optimum pitch angle, which generates the maximum output power, does not match the one for highest mechanical efficiency. The simulation results also show that floating offshore wind turbines operating under drag force is an interesting option to complement the conventional FOWT in a marine park since they can be intercalated reducing the wake effects and supplying additional power.

Keywords: Wind energy. Floating Offshore Wind Turbines. Pitch angle. Power generation. Drag forces.

INTRODUCTION

In this work, we will focus on offshore wind farms [1], of which it is relevant to point out that they have great potential in the present and near future. Specifically, we will focus on floating platform wind turbines, which allow the installation of wind farms in deeper waters than the rest, where there is higher wind potential and, in addition, lower foundation costs [2].

Additionally, we will talk about the control systems, whose purpose is to regulate the rotor power, control its rotation speed, and stop it if necessary [3]. Two types of control are distinguished depending on whether the entire blades are rotated about their

longitudinal axis (pitch) or if only one segment of the blades rotates, leaving another fixed to the rotor (stall) [4-6]. Among these two options, we focus our study on the pitch control effect on floating wind turbines to optimize the use of the wind resource, correcting the losses due to the rotor misalignment with the direction of the wind [7-8]. By varying the angle of attack of the wind on the blades, the force exerted on them varies and, therefore, the power generated by the rotor [9]. This control system increases the power extracted for wind speeds below the turbine-rated speed, or angles of attack less than the right angle, and keeps the speed constant in strong wind conditions [10]. In the event of a dangerously high wind speed, which puts the generator structure at risk, the blades rotate 90º (flag position) to stop them [11].

Several studies have been developed in the past analyzing the characteristics and performance of drag-floating offshore wind turbines [12-14]. Nevertheless, no specific work considers the effects of the pitch angle, which may improve the performance of the wind turbine.

THEORETICAL BACKGROUND

We calculate the electrical power available from the wind using the expression [15]:

$$P = \frac{1}{2}\rho A u^3 \tag{1}$$

Where ρ is the density of the fluid that moves the turbine, in this case, air, S is the surface swept by the rotor blades, and u is the average wind speed. If we take into account the angle, δ, that the rotor axis forms with the wind direction, a very influential fact when calculating the available power, equation 1 converts into:

$$P = \frac{1}{2}\rho A u^3 \cos\delta \tag{2}$$

The angle δ depends, in turn, on two other angles: the horizontal rotation angle, γ, and the vertical tilt angle, β, due to the waves [16]. We are especially interested in learning about the latter due to the relevance of the oscillating movement of floating wind turbines. We calculate the angle assuming periodic waves:

$$\tan\beta = 2\pi^2 \frac{H}{T^2 g}\cos\left(2\pi\frac{t}{T}\right) \tag{3}$$

With H being the height of the waves (amplitude of the wave), T is the period of the waves, and t is the time. On the other hand, we determine the angle γ from a complicated polynomial fit of degree 22 [17]:

$$\gamma = \sum_{i=0}^{22} a_i 10^{b_i} t_i \tag{4}$$

The coefficients *a* and *b* are characteristic of the offshore wind turbine location.

The δ angle can then be found as [18]:

$$\delta = \cos^{-1}\left(\frac{2\sin^2\gamma + \cos^2\gamma\cos^2\beta + \cos^2\gamma - \cos^2\gamma\left(\cos\beta - 1\right)^2}{2\left[\sin^2\gamma + \cos^2\gamma\cos^2\beta\right]^{1/2} + \left[\sin^2\gamma + \cos^2\gamma\right]^{1/2}}\right) \quad (5)$$

Since the wind speed undergoes high temporal variations, both in the short term in the form of gusts and throughout the year, describing a statistical distribution, we take the average hourly value of the wind throughout the year to carry out our calculations, which respond to a Weibull distribution. Mathematically:

$$F(u) = e^{-\frac{u}{c}k} \quad (6)$$

u is the instantaneous wind speed, *k* is a shape parameter related to the variability concerning the mean, and c is a shape parameter that refers to the mean annual wind speed. We can determine the wind speed probability density from the derivation of equation 6. The instantaneous wind speed relates to the mean value of wind speed over some time, Ū, as u=U/ Ū, where U accounts for the normalized wind speed.

Focusing on the wind turbine operation, we can analyze its performance from different characteristic curves. The most widely used represents power, torque and thrust against the specific blade tip speed (λ) or "tip speed ratio" [19]. The coefficient λ determines the ratio of linear speed at the tip of the blades, u, of a wind turbine in a given situation to the upstream wind speed, v; mathematically [20]:

$$\lambda = u/v \quad (7)$$

We can determine the power generation by a wind turbine from the C_p-λ curve, where C_p is the power coefficient:

$$C_p = \frac{P}{\frac{1}{2}\rho A u_o^2} \quad (8)$$

P is the power generated in the rotor, A is the area that the rotor sweeps and u_o is the wind speed at the height of the hub.

The moment coefficient relates the rotor torque (M) to the wind speed as:

$$C_T = \frac{M}{\frac{1}{2}\rho A u_o^2} = \frac{P/\Omega}{\frac{1}{2}\rho A u_o^2} \quad (9)$$

Ω is the rotor angular speed, equal to that of the blades and the hub.

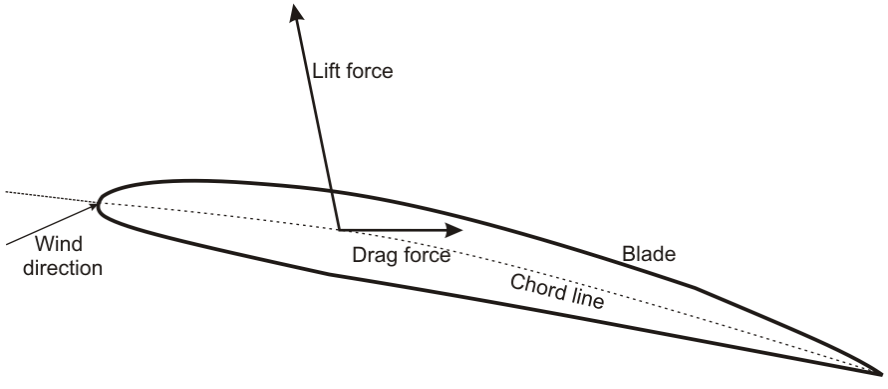

Figure 1 Schematic view of the wind turbine blade airfoil

In drag wind turbines, the torque derives from the action of the wind drag force (Figure 1); in such a case, we should apply the drag coefficient defined as:

$$C_D = \frac{D/l}{\frac{1}{2}\rho c u_o^2} \tag{10}$$

D is the drag force, c is the chord line length, and *l* is the unit length.

The drag force coefficient depends on the Reynolds number, which, on its way, depends on wind speed, air viscosity, υ, and rotor diameter, D. Mathematically:

$$\mathrm{Re} = \frac{u_o D}{\upsilon} \tag{11}$$

Figure 2 shows the evolution of the lift and drag coefficient as a function of the Reynolds number for variable wind angle of attack. We observe that the lift and drag coefficient increases with the wind angle of attack; however, the drag coefficient increases with the Reynolds number for a specific value of the angle of attack while the lift coefficient decreases. This situation is interesting since the wind dynamic force splits in two, lift and drag force; if one increases, the other decreases.

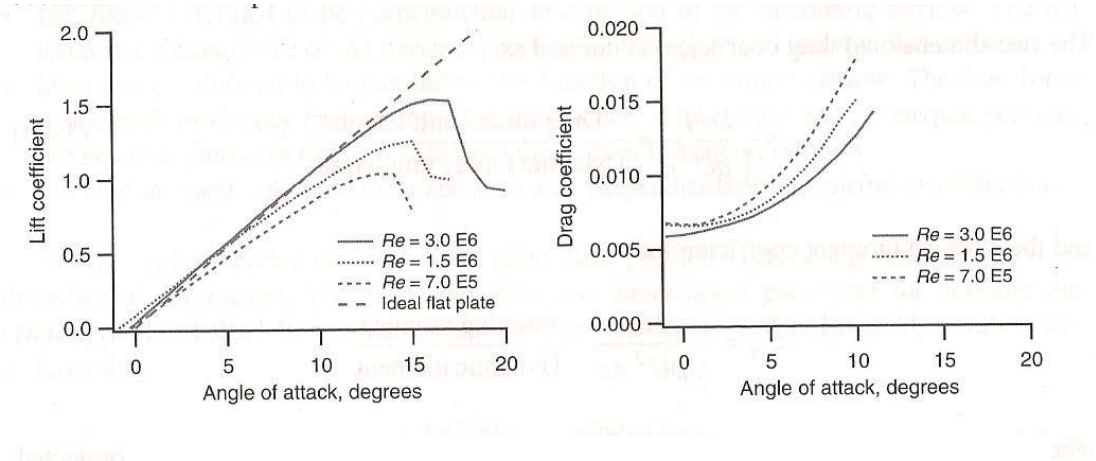

Figure 2 Evolution of lift and drag coefficient

Analyzing the wind dynamic force, we have:

$$F_w = \frac{1}{2}\rho A u_o^2 = F_l + F_d \tag{12}$$

Lift and drag forces can be expressed in terms of lift and drag coefficient:

$$F_l = \frac{1}{2} C_l \rho c u_o^2 l \; ; \; F_d = \frac{1}{2} C_d \rho c u_o^2 l \tag{13}$$

Combining equations 12 and 13:

$$C_l + C_d = \frac{A}{cl} \tag{14}$$

Since the rotor area and the blade and chord line length remain constant, the higher the lift coefficient, the lower the drag coefficient, and vice versa.

The rotor area depends on the blade length. Considering the hub diameter is negligible compared to the blade length, we have:

$$A = \frac{\pi}{2} L^2 \tag{15}$$

Therefore:

$$C_l + C_d = \frac{\pi}{2} \frac{L^2}{cl} \tag{16}$$

For a given blade length, the shorter the chord line, the higher the coefficient sum.

Analyzing Figure 2 and applying values to equation 16, we realize that the drag force represents the higher fraction of the wind dynamic force if the angle of attack and the Reynolds number are high. Reynolds number does not depend on blade shape and size; however, the angle of attack does. Therefore, the blade design in a drag wind turbine should show a sharp attack edge like in Figure 3 (right side).

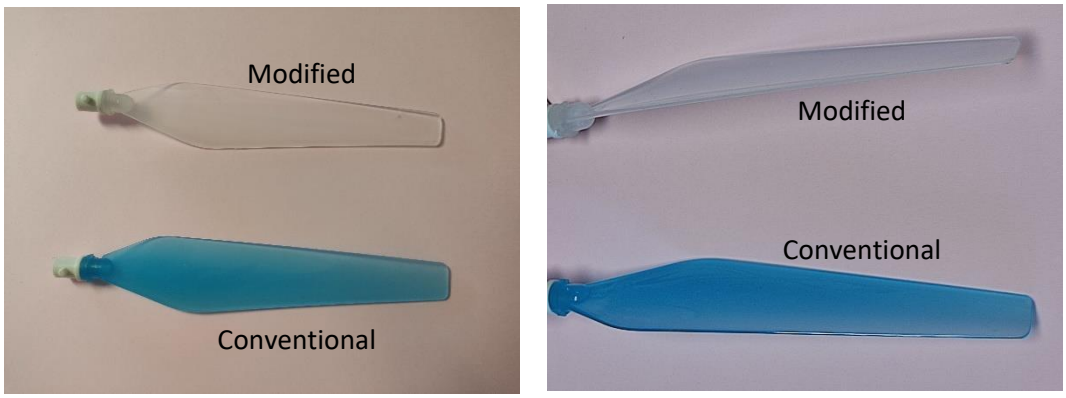

Figure 3 View of the conventional and modified blade for the testing wind turbine (left side: front view; right side: side view)

We observe that the wind turbine blade profile is similar looking at the front view; however, regarding the side view, there is a significant difference in the blade profile, which causes a better use of drag wind force.

Additionally, we can increase the wind angle of attack by modifying the pitch angle (Figure 4).

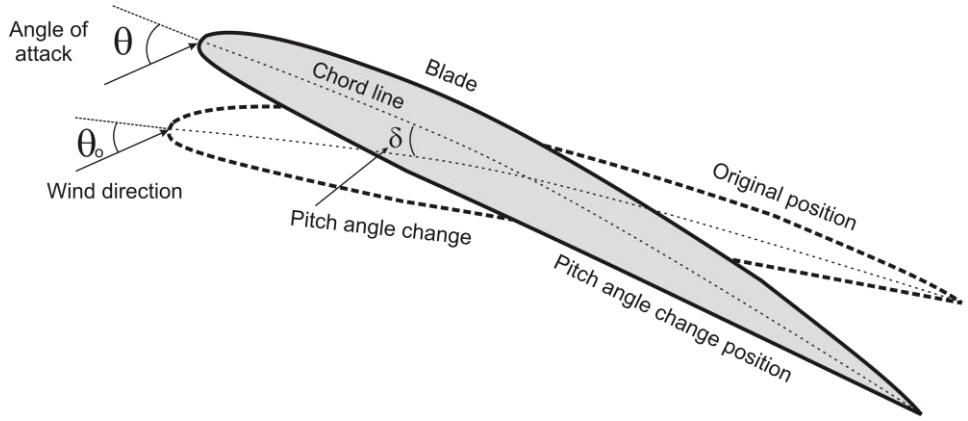

Figure 4 Schematic view of the wind turbine blade airfoil with pitch angle change

We observe the change in the wind angle of attack, from θ_o to θ, with the pitch angle change, δ.

Combining a sharp blade attack edge with a pitch angle change, we modify the angle of attack to the appropriate value to increase the drag-to-lift force ratio.

EXPERIMENTAL RESULTS

In this section, we present the results of experimental tests conducted to maximize the output power of a drag wind turbine as a function of the pitch angle. Experimental tests run on a lab wind turbine model, reproducing the characteristics of commercial wind turbines at a reduced scale. We modified the wind turbine blades shape to accommodate the design to a more effective use of drag force to the detriment of the lift one.

The designed wind turbine blade is built in molded polycarbonate, having a length of 12.137 cm and a chord line of 2.944 cm. Three identical blades were attached to a micro wind turbine articulated hub, which allows modifying the pitch angle in a range up to 15º in 1º step. We put the micro wind turbine in a 50 cm diameter wind tunnel to run tests. We simulate the wind stream with a commercial fan of 150 W power. The fan generates a maximum wind speed of 7.5 m/s.

The first group of tests run for characterizing the wind turbine rotor, specifically the power coefficient, Cp. We measure the output power for wind speed ranges between 2.55 m/s and 7.5 m/s. Wind speed is measured with a precision hot wire anemometer of 0.01 m/s accuracy. Power is measured with a professional power analyzer of 1 mW accuracy. We show the power coefficient for the tested prototype in Table 1.

Table 1 Power coefficient for the tested prototype at variable wind speed

Wind speed (m/s)	Wind power (W)	Wind turbine output power (W)	C_p
7.50	594.316	219.671	0.370
7.45	582.509	214.612	0.368
7.00	483.201	176.186	0.365
6.40	369.295	136.973	0.371

6.00	304.290	112.445	0.370
5.40	221.827	81.173	0.366
4.85	160.716	59.501	0.370
4.25	108.144	39.649	0.367
3.55	63.026	23.068	0.366
3.05	39.970	14.524	0.363
2.55	23.359	8.727	0.374

The average value for the power coefficient is 0.368 with a standard deviation of 0.003, which is an excellent result proving the quality of the designed wind turbine blade. On the other hand, if we compare the power coefficient value with those for highly efficient large commercial wind turbines, the deviation is less than 8%, reinforcing the statement of high-quality wind turbine blade design.

We run a second group of tests to determine the influence of the pitch angle on the wind turbine performance. Since we simulate the behavior of a floating offshore wind turbine, we run the tests for variable wind turbine tilt and pitch angle. We measure the wind turbine tilt with a 0.1 º precision inclinometer attached to the stand. We determine the pitch angle with a pitch angle meter of 0.1º accuracy attached to the wind turbine blade.

Figure 5 shows the evolution of the maximum power for the tested drag wind turbine for different tilt angles of the floating wind turbine with the pitch angle. The larger circles indicate the maximum generated power value by the prototype for a mast tilt angle given value. The area shaded in yellow corresponds to the highest concentration of test points for maximum power for the studied cases. We observe that only the case for 17º tilt leaves the zone.

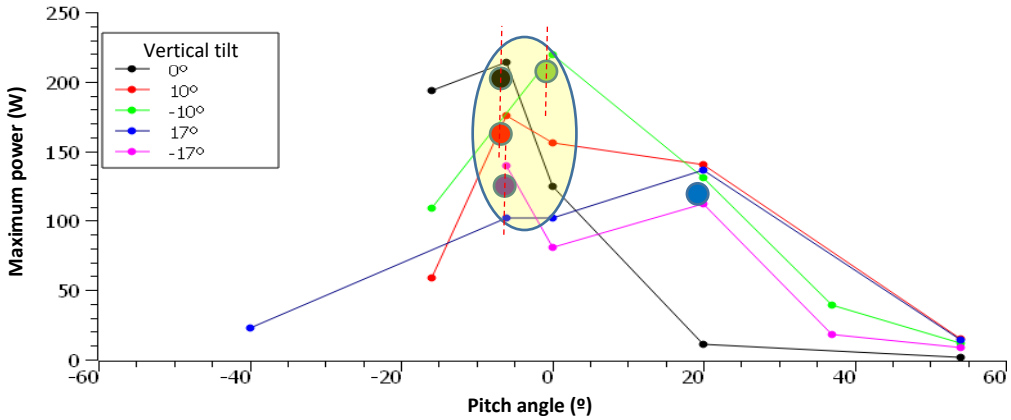

Figure 5. Evolution of the maximum output power of a drag floating wind turbine for different tilt angles and variable pitch

On the other hand, we realize that the maximum powers concentrate at pitch angles in the range of -1.4º to -7.1º, centered at -4º, in good agreement with predicted values. We also highlight that the power generated decreases for increasing angles. It is also remarkable that we may achieve higher power values at intermediate angles, provided the instrumentation accuracy improves.

The accuracy of the proposed model is evaluated from the comparative analysis between theoretical values and experimental data. Replacing data from our prototype in equation 16, we have:

$$C_l + C_d = \frac{\pi}{2}\frac{(0.12137)^2}{(0.02944)} = 0.786 \qquad (17)$$

Applying this value to graph of figure 2, we obtain the wind angle of attack that matches equation 17, resulting θ=3.8º. Now, averaging the values for maximum power from experimental tests, we obtain θ=4.2º. Therefore, theoretical value deviates from experimental data 0.4º.

The third group of tests focuses on evaluating the mechanical efficiency of the prototype. Figure 6 shows the results from experimental tests.

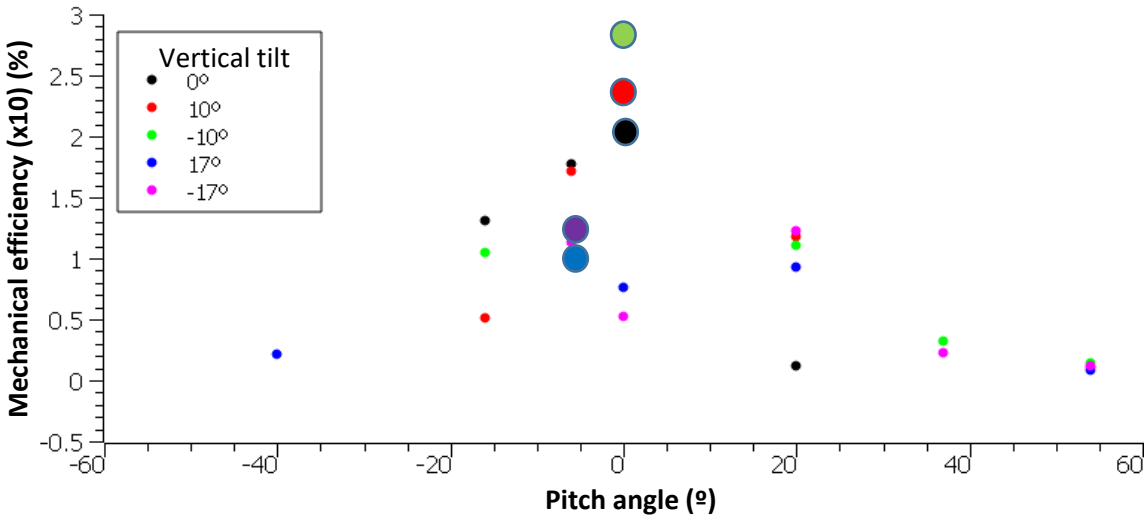

Figure 6. Evolution of the mechanical efficiency of a drag floating offshore wind turbine for variable tilt angle and pitch

In Figure 6, we observe that the most efficient position is at 0º pitch angle for all inclinations except for +/-17º, whose most efficient position is -6º. The efficiency drops as pitch angle increases, reaching a mechanical efficiency as low as 0.1% for the highest pitch angles. The highest mechanical efficiency is near 30%, achieved at -10º tilt angle and 0º pitch angle. The mechanical efficiencies are low, while the Cp is high; this leads to conclude that the efficiency loss is due to the electric generator and not to the blade design.

CONCLUSIONS

A new wind turbine blade is designed and built for using drag forces instead of lift ones. The proposed prototype shows a good power coefficient, C_p=0.38, which is in the range of highly efficient commercial wind turbines, within an 8% deviation.

Experimental tests show that the prototype operates at maximum output power for a pitch angle between -1.4º and -7.1º, with an average peak point for a pitch angle of -4º, in good agreement with the predicted value from theoretical calculation, within a 0.4º deviation.

The prototype's mechanical efficiency is poor due to the low quality of the electric generator. Nevertheless, the prototype may achieve a near 30% efficiency at optimum operating conditions, comparable to other mechanical energy converters.

The high agreement between experimental tests and theoretical predictions proves the quality of the prototype design and its suitability for drag force operation. The results obtained from the developed study show a promising future for drag-force wind turbines and their application to floating offshore wind parks.

REFERENCES

[1] L. Castro-Santos & V. Diaz-Casas, (Eds.). Floating offshore wind farms (p. 204). Cham, Switzerland: Springer International Publishing (2016).

[2] V. Pérez Alonso, Caracterización de Turbinas Flotantes. Comparación con Aerogeneradores Terrestres, Grupo de Energías Renovables. Facultad de Físicas. Universidad Complutense de Madrid. Trabajo Fin de Máster. 2020.

[3] S. D. L. SALLE, D. Reardon, W. E. Leithead & M. J. GRlMBLE, Review of wind turbine control. International Journal of Control, Volume 52, Issue 6, pages 1295-1310 (1990).

[4] Apata, O., & Oyedokun, D. T. O. (2020). An overview of control techniques for wind turbine systems. *Scientific African*, *10*, e00566.

[5] Bianchi, F. D., De Battista, H., & Mantz, R. J. (2007). *Wind turbine control systems: principles, modelling and gain scheduling design* (Vol. 19). London: Springer.

[6] SALLE, S. D. L., Reardon, D., Leithead, W. E., & GRlMBLE, M. J. (1990). Review of wind turbine control. *International Journal of control*, *52*(6), 1295-1310.

[7] Namik, H., & Stol, K. (2010). Individual blade pitch control of floating offshore wind turbines. *Wind Energy: An International Journal for Progress and Applications in Wind Power Conversion Technology*, *13*(1), 74-85.

[8] Namik, H., & Stol, K. (2013). Individual blade pitch control of a spar-buoy floating wind turbine. *IEEE transactions on control systems technology*, *22*(1), 214-223.

[9] Fazylova, A., Tultayev, B., Iliev, T., Stoyanov, I., & Beloev, I. (2023). Development of a Control Unit for the Angle of Attack of a Vertically Axial Wind Turbine. *Energies*, *16*(13), 5202.

[10] Leithead, W. E., & Connor, B. (2000). Control of variable speed wind turbines: Design task. *International Journal of Control*, *73*(13), 1189-1212.

[11] Aubrun, S., Leroy, A., & Devinant, P. (2017). A review of wind turbine-oriented active flow control strategies. *Experiments in Fluids*, *58*, 1-21.

[12] J. Orszaghova, P. H. Taylor, H. A. Wolgamot, F. J. Madsen, A. M. Pegalajar-Jurado & H. Bredmose, Wave-and drag-driven subharmonic responses of a floating wind turbine. Journal of Fluid Mechanics, Volume 929 (2021).

[13] L.Zhang, W. Shi, M. Karimirad, C. Michailides & Z. Jiang, Second-order hydrodynamic effects on the response of three semisubmersible floating offshore wind turbines. Ocean Engineering, Volume 207, 107371 (2020).

[14] D. Yin, E. Passano, F. Jiang, H. Lie, J.u, N.Ye & B. J. Leira, State-of-the-Art Review of Vortex-Induced Motions of Floating Offshore Wind Turbine Structures. Journal of Marine Science and Engineering, Volume 10, Issue 8, page 1021 (2022).

[15] Manwell, J. F., McGowan, J. G., & Rogers, A. L. (2010). Wind energy explained: theory, design and application. John Wiley & Sons.

[16] Armenta-Déu. C., Racouchot, N. (2021) Modelling of Wind-Wave Misalignment for Floating Off-Shore Wind Turbine. Journal of Offshore Structure and Technology, Volume 8, Issue 2, pages 18-35

[17] Armenta-Déu, C. (2023) A Model to Predict Angular Phase Shift between Wind and Waves for FOWT Applications. Journal of Offshore Structure and Technology, Volume 10, Issue 11, pages 1-12

[18] Armenta-Déu, C., Lomo, J. (2022) Wave Effects on the Performance of Giant Floating Offshore Wind Turbines. Journal of Offshore Structure and Technology, Volume 9, Issue 2, pages 6-17

[19] Burton, T., Jenkins, N., Sharpe, D., & Bossanyi, E. (2011). Wind energy handbook. John Wiley & Sons.

[20] Stoevesandt, B., Schepers, G., Fuglsang, P., & Sun, Y. (Eds.). (2022). Handbook of wind energy aerodynamics. Springer Nature.